Supporting Information

Chiral Discrimination of Diamines by a Binaphthalene Bridged Porphyrin dimer

Wenxin Lu, Huifang Yang, Xinyao Li, Chiming Wang, Xiaopeng Zhan, Dongdong Qi, Yongzhong Bian and Jianzhuang Jiang

Beijing Key Laboratory for Science and Application of Functional Molecular and Crystalline Materials, Department of Chemistry, University of Science and Technology Beijing, Beijing 100083, China

Content

Chemicals and Instruments

Column chromatography was carried out on silica gel (200-300 mesh, Qingdao Ocean Chemicals) with the indicated eluent. Toluene and N,N-dimethylformamide (DMF) were freshly distilled from CaH_2 under nitrogen. 5-(4-hydroxyphenyl)-10,15,20-tris(4-*tert*-butylphenyl)porphyrin (Zn(TTBPP)) [S1] was prepared according to the published procedures. All other reagents and solvents were used as received.

^{1}H NMR spectra were recorded on a Bruker DPX 400 spectrometer (400 MHz) in $CDCl_3$ and the chemical shifts were reported relative to internal $SiMe_4$. MALDI-TOF mass spectra were taken on a Bruker Microflex^{TM} LRF spectrometer with dithranol as the matrix. Elemental analyses were performed on an Elementar Vavio El III elemental analyzer. Electronic absorption spectra were recorded on a Lambda 750 spectrophotometer. CD spectra were recorded on a JASCO J-1500 spectropolarimeter.

Synthetic scheme of (*R*)-/(*S*)-H1.

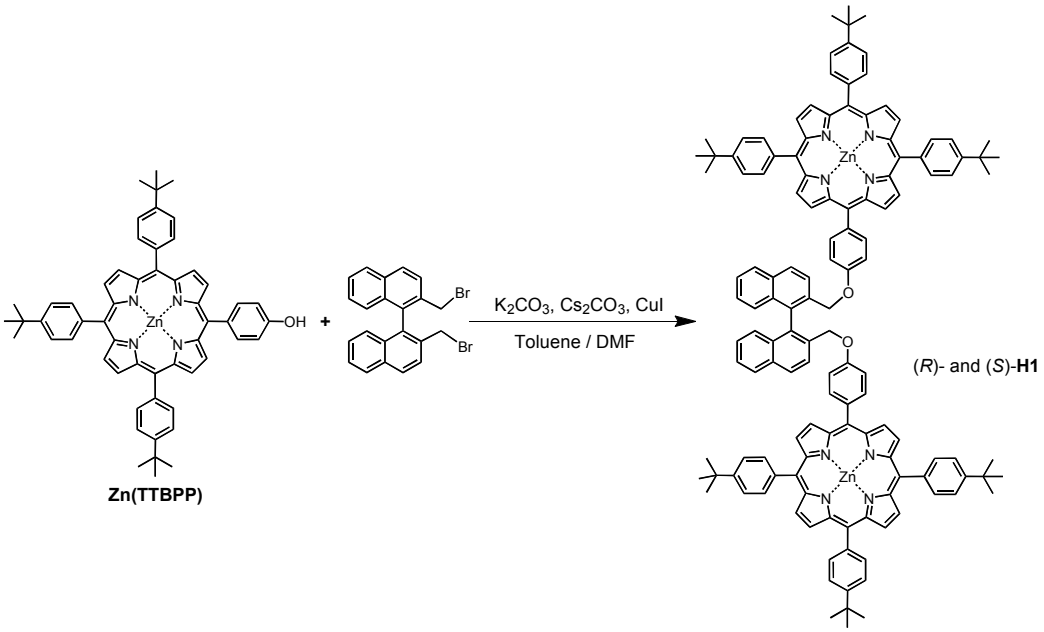

Zn(TTBPP)

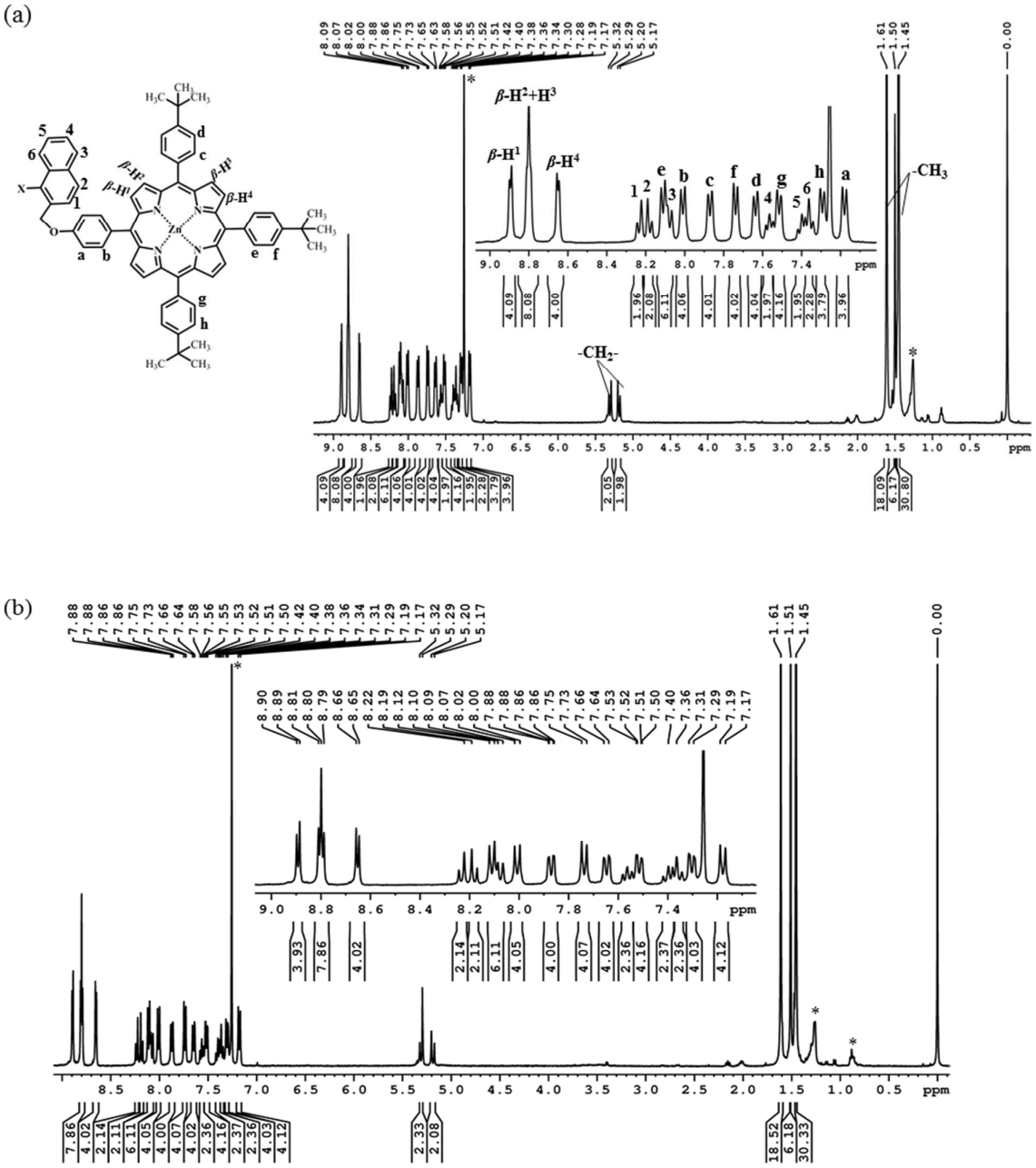

Figure S1. ^{1}H NMR spectrum of (a) (*R*)-**H1** and (b) (*S*)-**H1** in $CDCl_3$ at 293 K. * indicate the residual solvent signals.

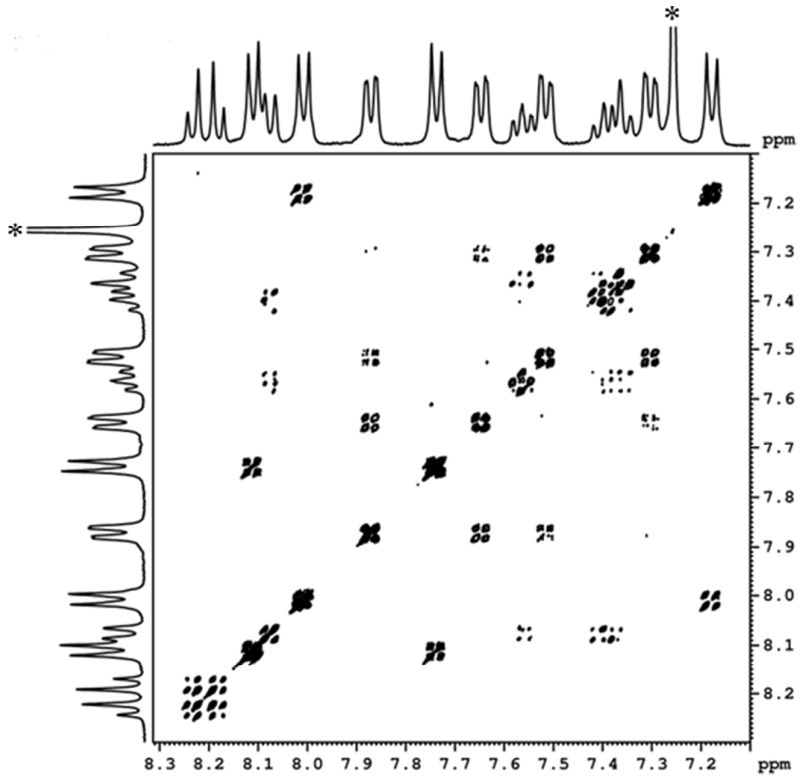

Figure S2. ^{1}H-^{1}H COSY spectra of (*S*)-**H1** in $CDCl_3$ at 293 K. * indicate the residual solvent signals.

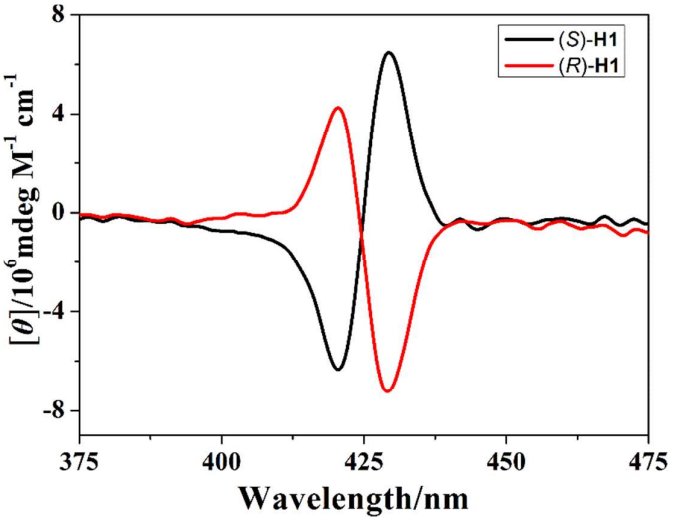

Figure S3. CD spectra of (*S*)-**H1** (black) and (*R*)-**H1** (red) in $CHCl_3$ at 298 K.

UV-Vis Spectrophotometric Titration.

Method for Evaluation of Association Constants (K_{assoc})

The association constant K_{assoc} for the 1:1 complexes was derived by using the non-linear curve fitting based on the equation:

$$\Delta Abs = (A_\infty(1+K_{assoc}[G]+K_{assoc}[H]) - (A_\infty^2(K_{assoc}[G]+K_{assoc}[H]+1)^2-4K_{assoc}^2[H]*[G] A_\infty^2)^{0.5})/2K_{assoc}[H]$$

Where [G] and [H] represent $[Guest]_{total}$ and $[Host]_{total}$, respectively; A_∞ denotes ΔAbs at 100% complexation; A_∞ and K_{assoc} are parameters. [S2]

For the 1:2 complexes, the apparent association constant K_{assoc} was evaluated from the same equation, but $[H] = 2*[Host]_{total}$. [S2]

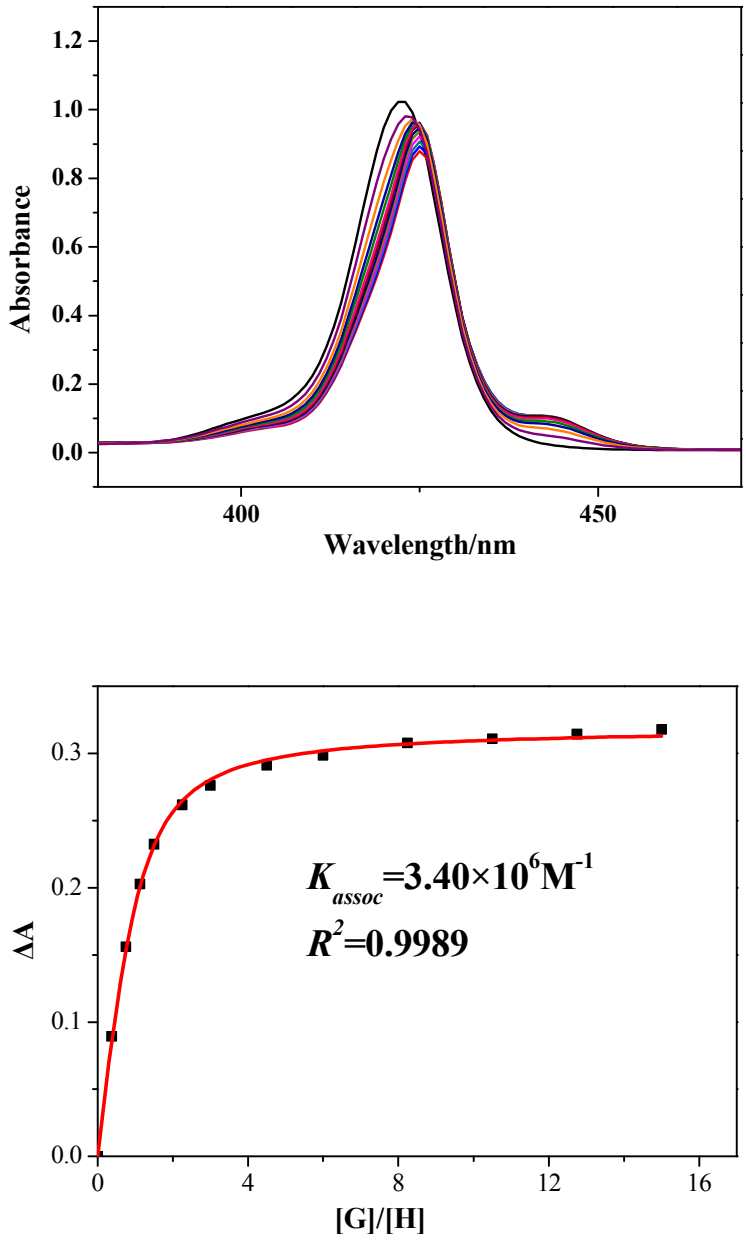

Figure S4. (a) Spectral change upon titration of (*R*)-**H1** with (*S*)-DACH in $CHCl_3$ at 298 K. (b) Changes in ΔA at 420 nm for evaluating K_{assoc}, the solid line represents the non-liner least square fit for 1:1 complexation. [(*R*)-**H1**] = 1.0 × 10^{-6} M; (*S*)-DACH /[(*R*)-**H1**] = 0−15.

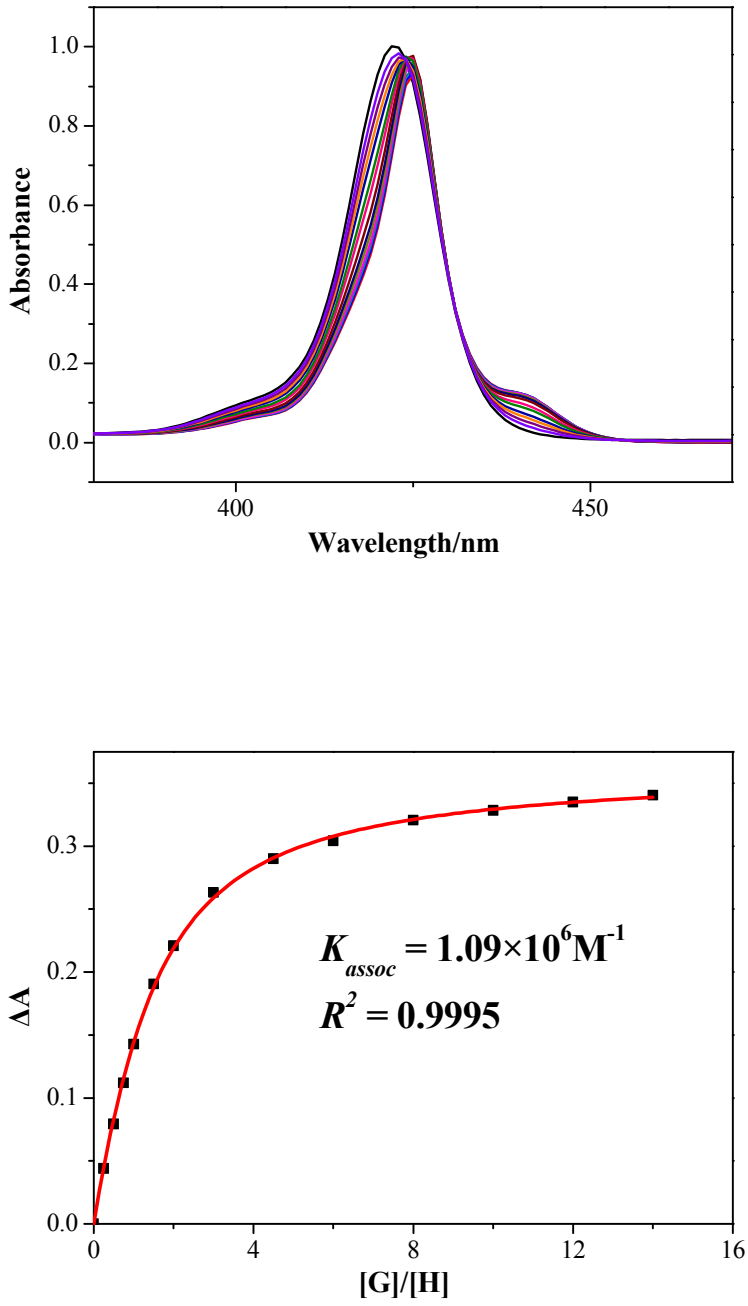

Figure S5. (a) Spectral change upon titration of (*R*)-**H1** with (*R*)-PPDA in $CHCl_3$ at 298 K. (b) Changes in ΔA at 420 nm for evaluating K_{assoc}, the solid line represents the non-liner least square fit for 1:1 complexation. [(*R*)-**H1**] = 1.0×10^{-6} M; (*R*)-PPDA/[(*R*)-**H1**] = 0−15.

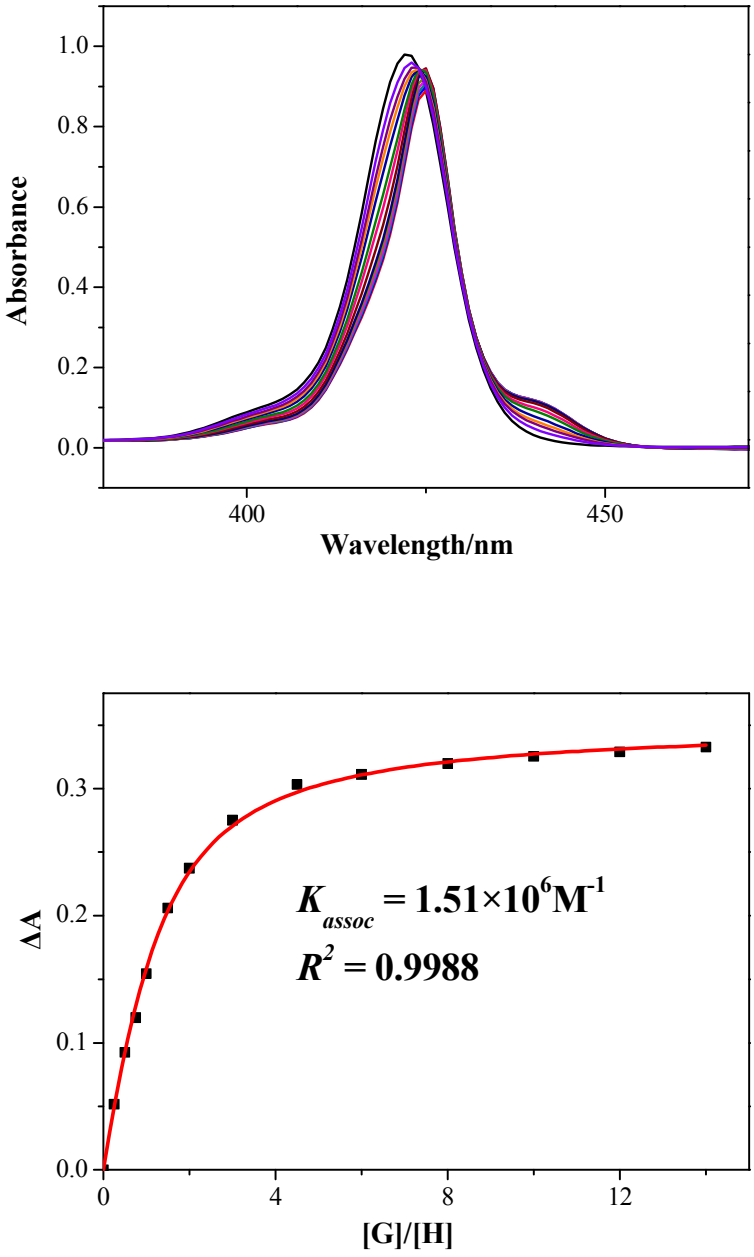

Figure S6. (a) Spectral change upon titration of (*R*)-**H1** with (*S*)-PPDA in $CHCl_3$ at 298 K. (b) Changes in ΔA at 420 nm for evaluating K_{assoc}, the solid line represents the non-liner least square fit for 1:1 complexation. [(*R*)-**H1**] = 1.0×10^{-6} M; (*S*)-PPDA/[(*R*)-**H1**] = 0−15.

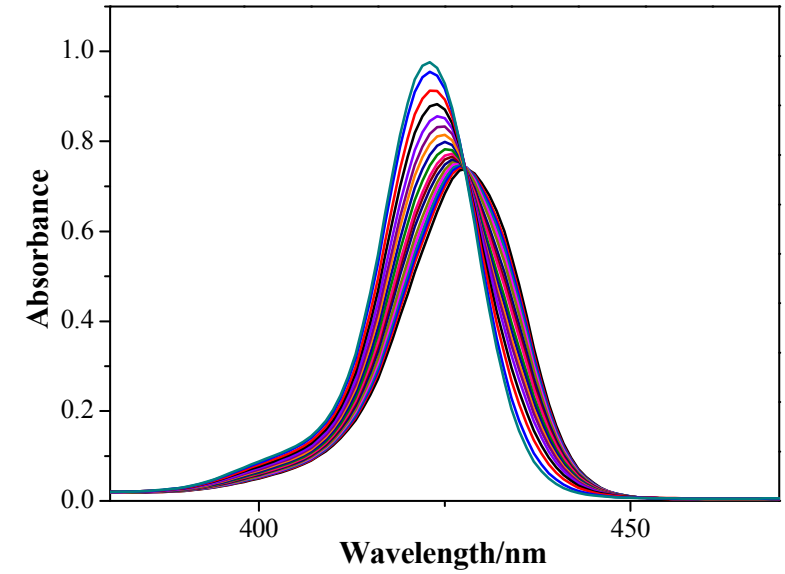

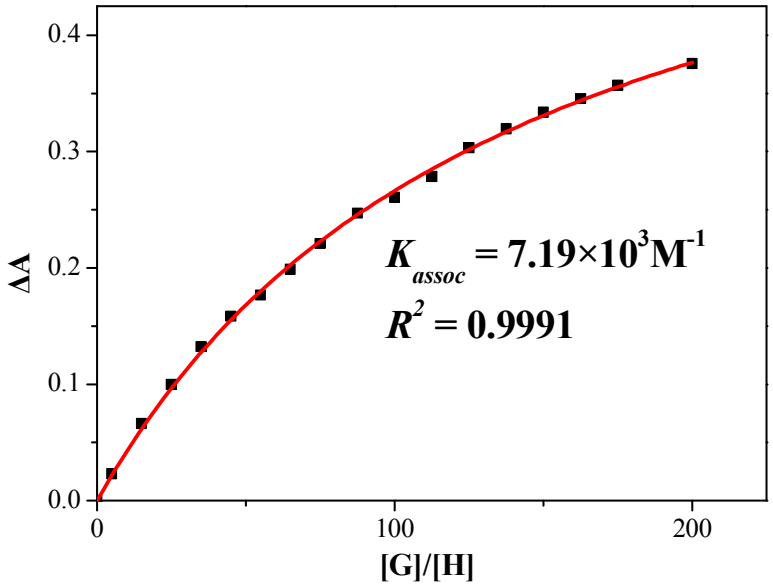

Figure S7. (a) Spectral change upon titration of (*R*)-**H1** with (*R*)-DPEA in $CHCl_3$ at 298 K. (b) Changes in ΔA at 420 nm for evaluating K_{assoc}, the solid line represents the non-liner least square fit for 1:2 complexation. [(*R*)-**H1**] = 1.0 × 10^{-6} M; (*R*)-DPEA/[(*R*)-**H1**] = 0−200.

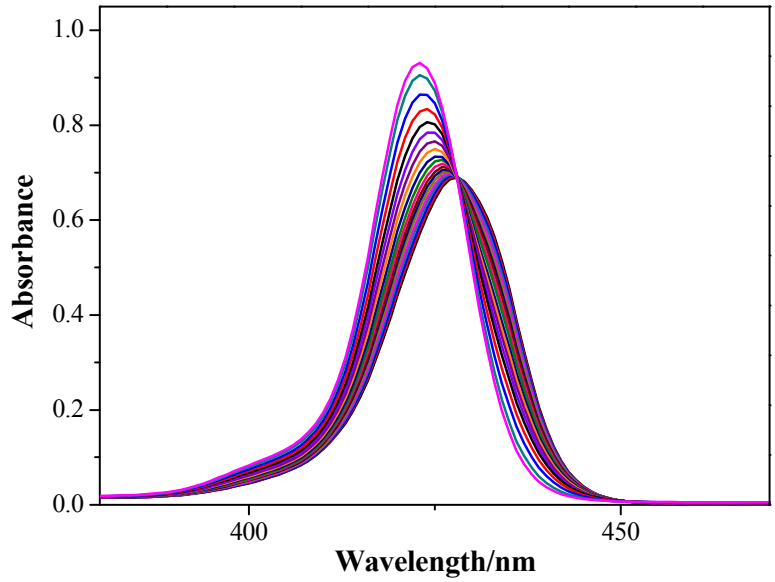

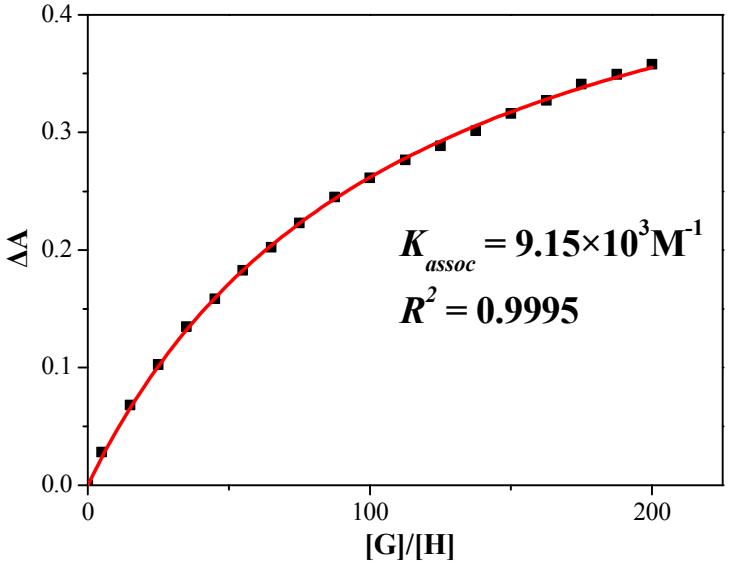

Figure S8. (a) Spectral change upon titration of (*R*)-**H1** with (*S*)-DPEA in $CHCl_3$ at 298 K. (b) Changes in ΔA at 420 nm for evaluating K_{assoc}, the solid line represents the non-liner least square fit for 1:2 complexation. [(*R*)-**H1**] = 1.0×10^{-6} M; (*S*)-DPEA/[(*R*)-**H1**] = 0–200.

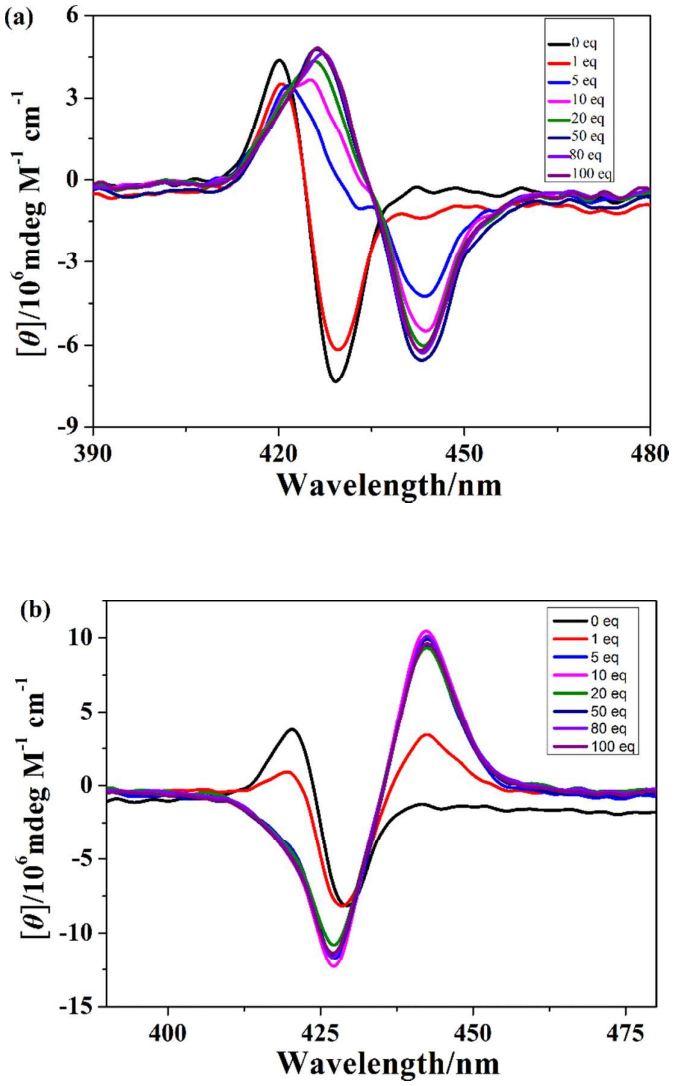

Figure S9. CD spectral change upon titration of (*R*)-**H1** with (*R*)-DACH (a) and (*S*)-DACH (b) in $CHCl_3$ at 298 K, [(*R*)-**H1**] = 1.0×10^{-6} M; DACH/[(*R*)-**H1**] = 0−100.

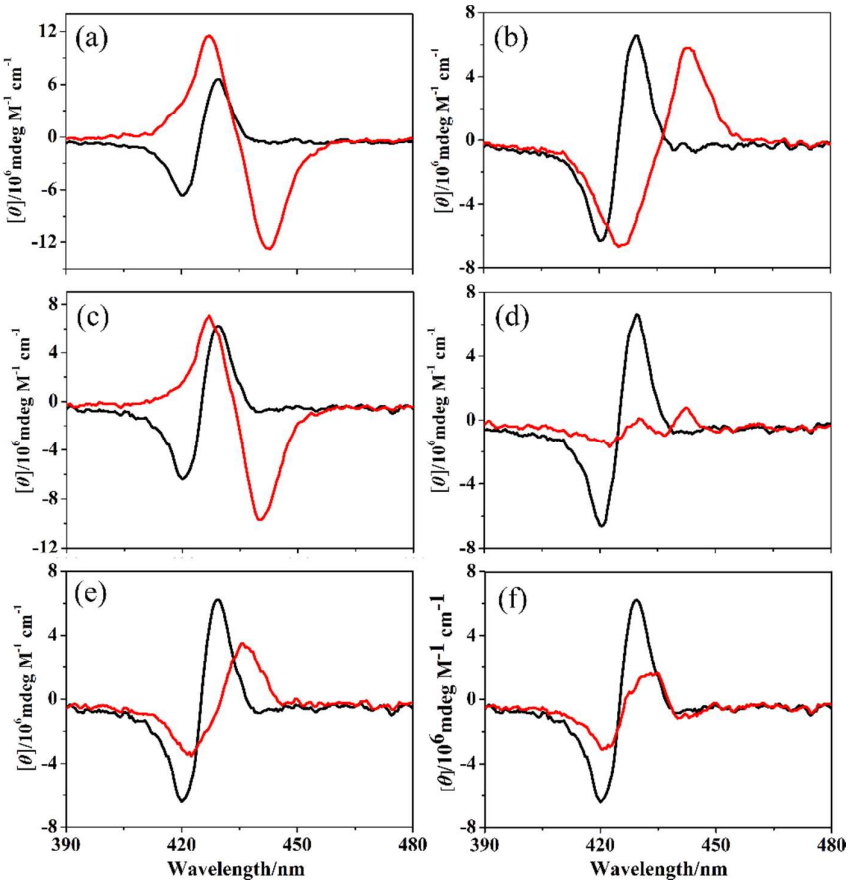

Figure S10. CD spectra of (*S*)-**H1** before (black) and after (red) the addition of: (a) (*R*)-DACH (20 equiv), (b) (*S*)-DACH (20 equiv), (c) (*R*)-PPDA (20 equiv), (d) (*S*)-PPDA (20 equiv), (e) (*R*)-DPEA (200 equiv), and (f) (*S*)-DPEA (200 equiv).

Computational details: DFT calculations on the optimization of geometric molecular structures were performed at DFT method at the B97D/6-31G(D) level using Gaussian 09 (*Version D.01*) program. [S3] The torsion angle (*Φ*) between the two chromophores is the spatial angel of C15-C5-C5′-C15′. The interchromophoric distance is the distance of Zn-Zn.

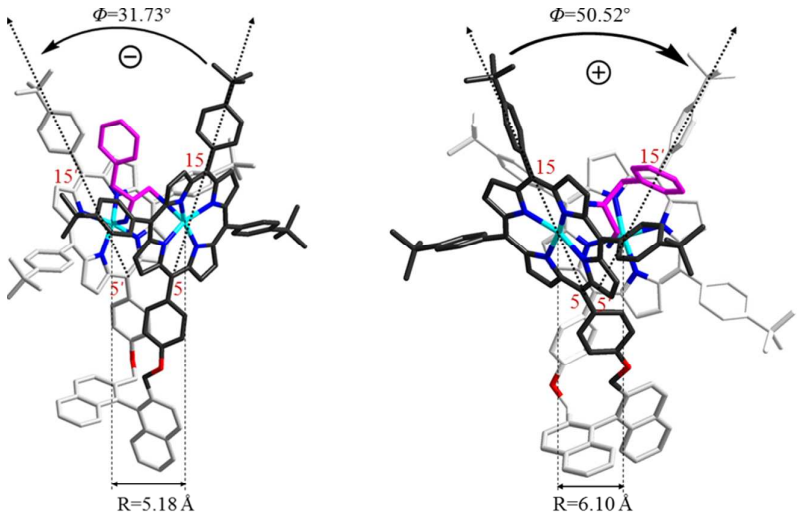

Figure S11. Optimized molecular structures of (*S*)-**H1**⊃(*R*)-PPDA and (*S*)-**H1**⊃(*S*)-PPDA by DFT method at the B97D/6-31G(D) level. The torsion angle *Φ* is the spatial angel of C15-C5-C5′-C15′; the interchromophoric distance is the Zn-Zn distance in Å.

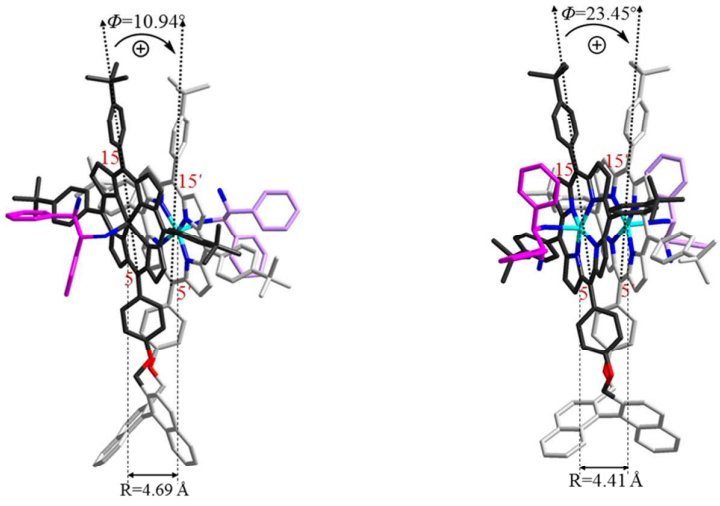

(*S*)-**H1**@[(*R*)-DPEA]$_2$ (*S*)-**H1**@[(*S*)-DPEA]$_2$

Figure S12. Optimized molecular structures of (*S*)-**H1**@[(*R*)-DPEA]$_2$ and (*S*)-**H1**@[(*S*)-DPEA]$_2$ by DFT method at the B97D/6-31G(D) level. The torsion angle Φ is the spatial angel of C15-C5- C5′-C15′; the interchromophoric distance is the Zn-Zn distance in Å.

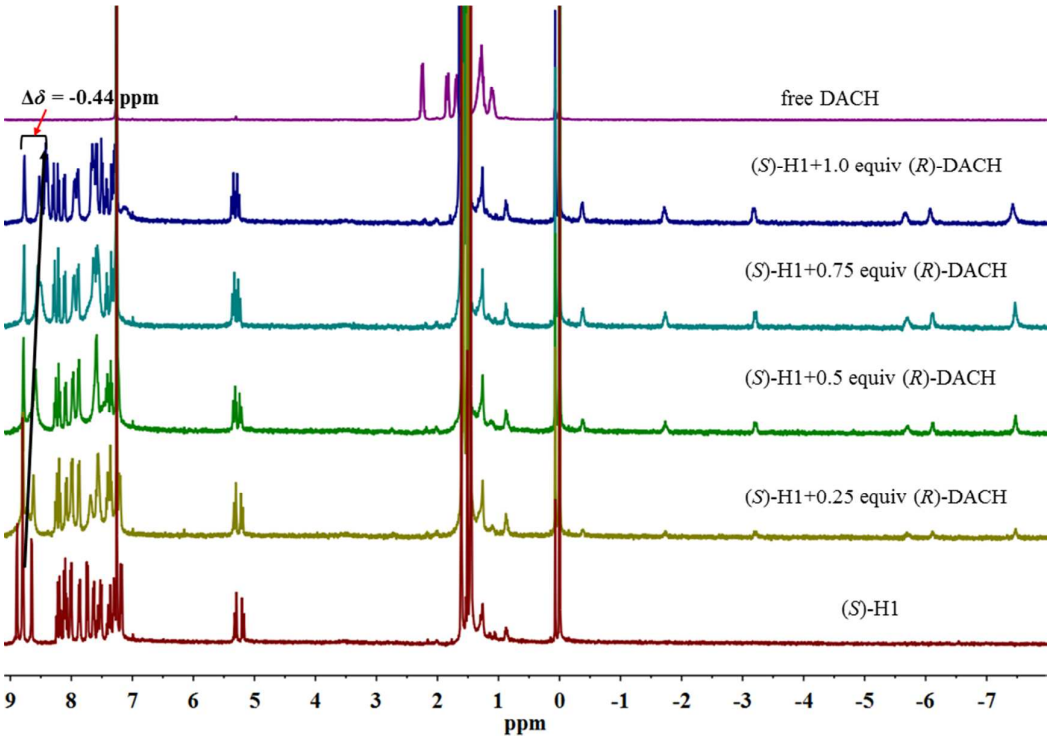

Figure S13. ^{1}H NMR titration spectra of (*S*)-**H1** (0.75 mM) with (*R*)-DACH (0.0-1.0 equiv, 0.25 equiv additions) at 298 K in $CDCl_3$.

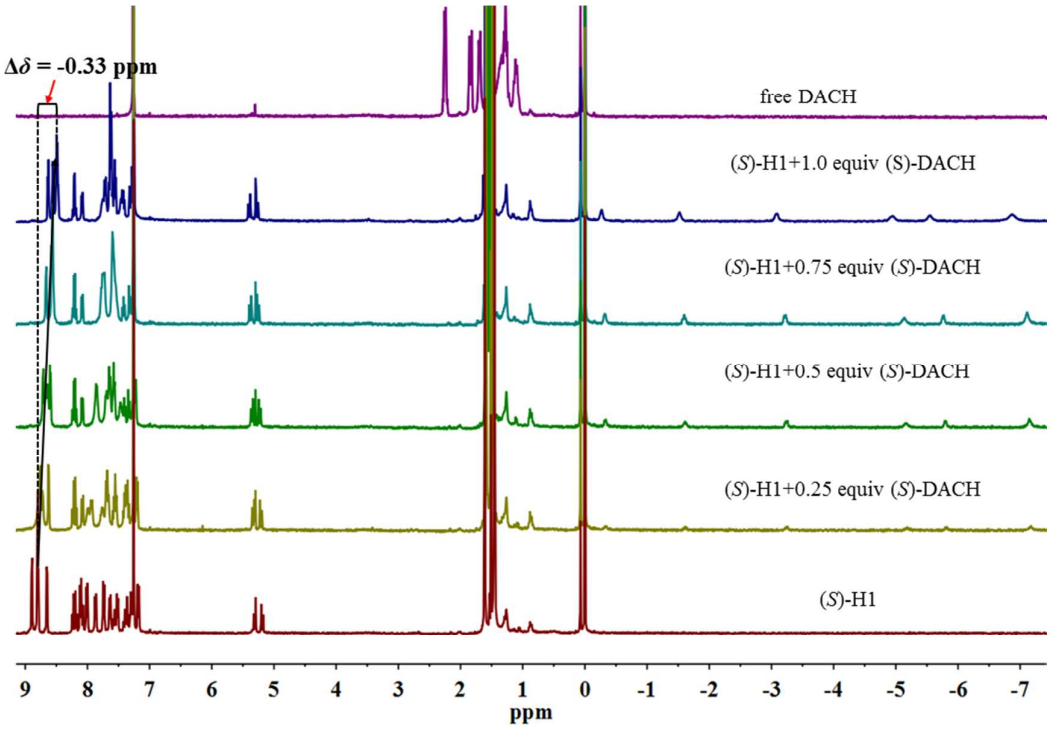

Figure S14. ^{1}H NMR titration spectra of (*S*)-**H1** (0.75 mM) with (*S*)-DACH (0.0-1.0 equiv, 0.25 equiv additions) at 298 K in $CDCl_3$.

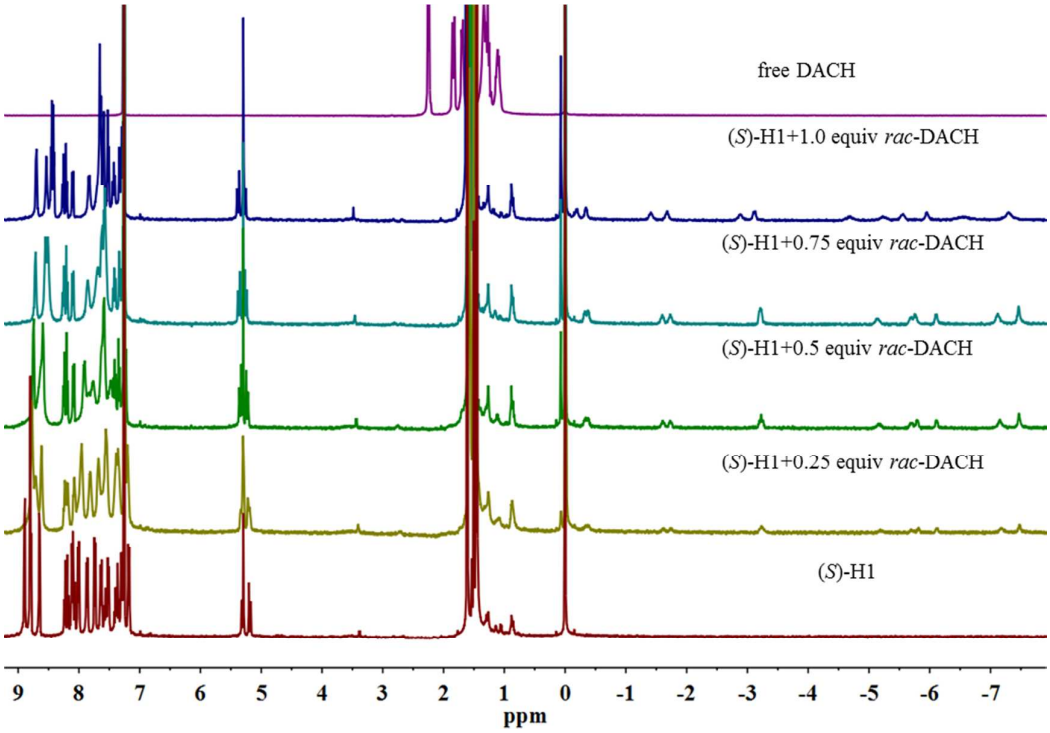

Figure S15. ^{1}H NMR titration spectra of (*S*)-**H1** (0.75 mM) with *rac*-DACH (0.0-1.0 equiv, 0.25 equiv additions) at 298 K in $CDCl_3$.

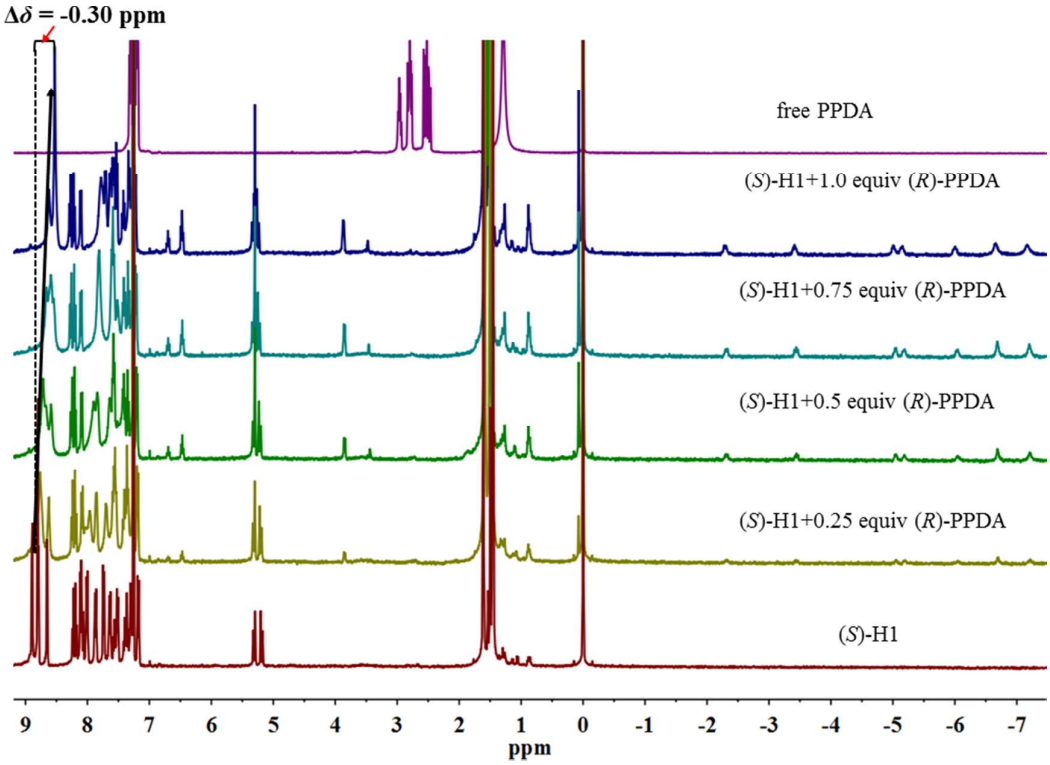

Figure S16. ^{1}H NMR titration spectra of (*S*)-**H1** (0.75mM) with (*R*)-PPDA (0.0-1.0 equiv, 0.25 equiv additions) at 298 K in $CDCl_3$.

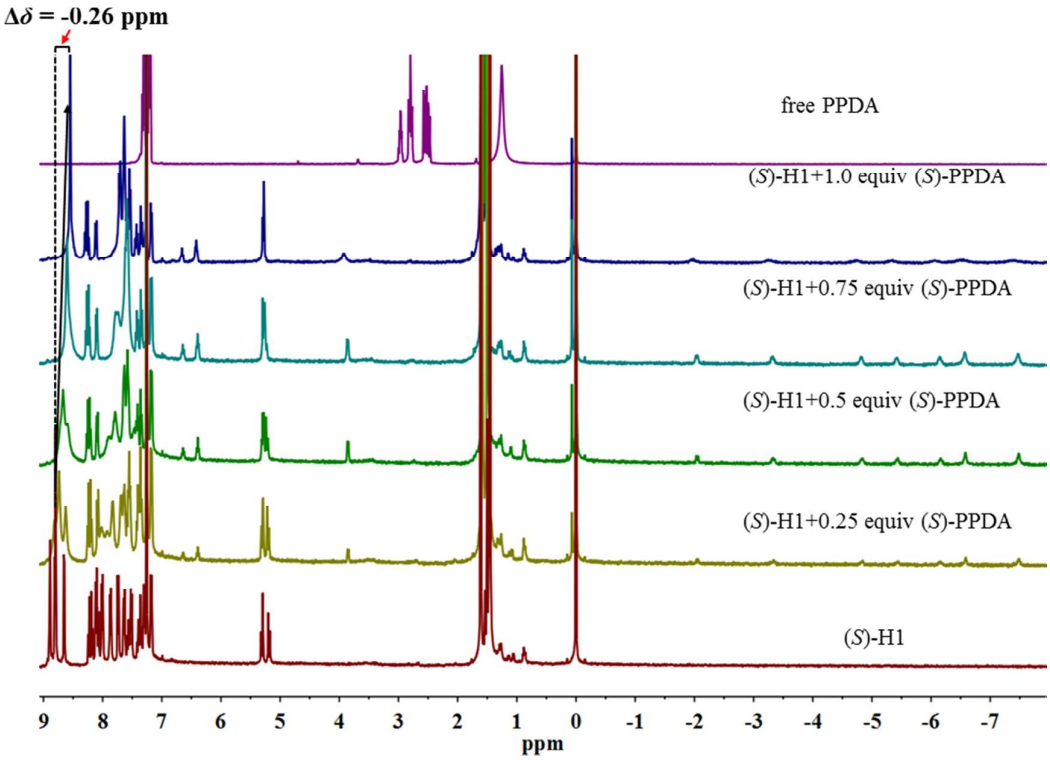

Figure S17. ^{1}H NMR titration spectra of (*S*)-**H1** (0.75 mM) with (*S*)-PPDA (0.0-1.0 equiv, 0.25 equiv additions) at 298 K in $CDCl_3$.

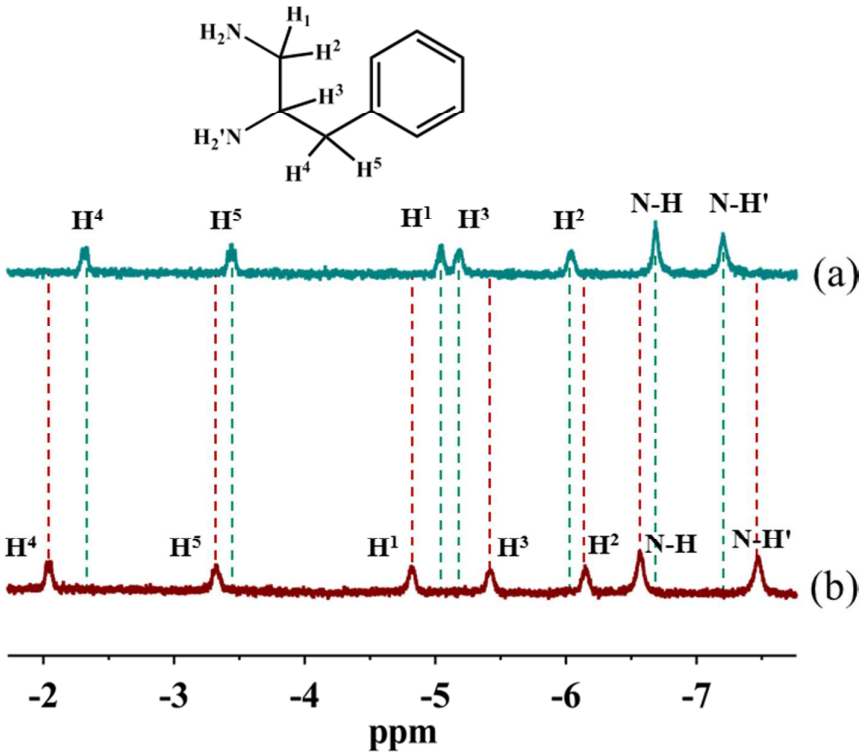

FigureS 18. Selected region of 400 MHz ^{1}H NMR spectra in the presence of (*S*)-**H1** (0.75 mM) in $CDCl_3$ at 293K: (a) (*S*)-PPDA (0.75 equiv); (b) (*R*)-PPDA (0.75 equiv).

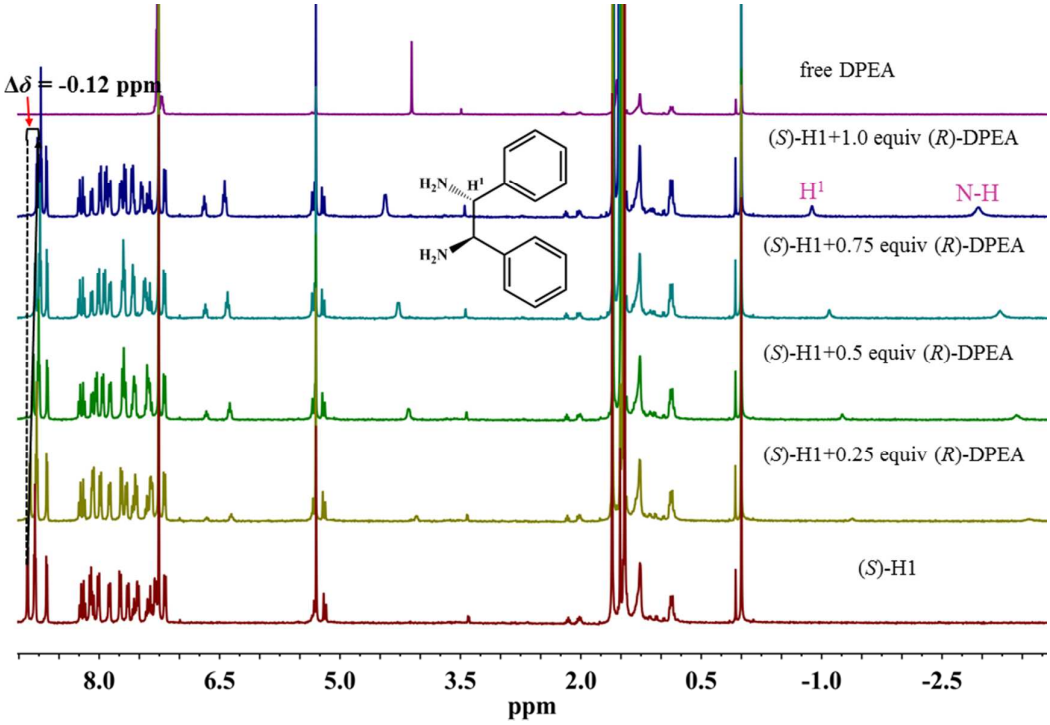

Figure S19. ^{1}H NMR titration spectra of (*S*)-**H1** (0.75 mM) with (*R*)-DPEA (0.0-1.0 equiv, 0.25 equiv additions) at 298 K in $CDCl_3$.

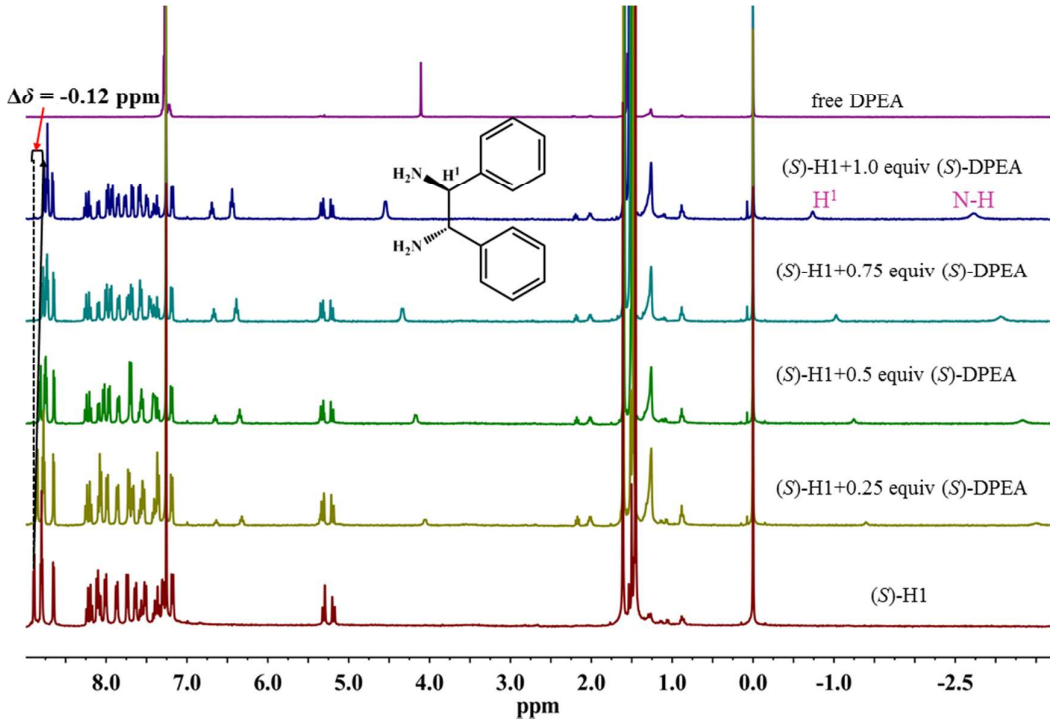

Figure S20. ^{1}H NMR titration spectra of (*S*)-**H1** (0.75 mM) with (*S*)-DPEA (0.0-1.0 equiv, 0.25 equiv additions) at 298 K in $CDCl_3$.

Table S1. CD data of (*S*)-**H1** with chiral 1,2-diamines.[a]

Compounds	λ ($\Delta\varepsilon$) nm($mol^{-1}\cdot L\cdot cm^{-1}$)		A_{CD} ($mol^{-1}\cdot L\cdot cm^{-1}$)
	1st	2nd	
(*S*)-**H1**	430 (+200)	420 (-202)	402
(*S*)-**H1**⊃(*R*)-DACH	443 (-387)	428 (+349)	-736
(*S*)-**H1**⊃(*S*)-DACH	444 (+176)	425 (-203)	379
(*S*)-**H1**⊃(*R*)-PPDA	440 (-294)	427 (+214)	-508
(*S*)-**H1**⊃(*S*)-PPDA	443 (+24)	423 (-52)	76
(*S*)-**H1**@[(*R*)-DPEA]$_2$	436 (+106)	423 (-107)	213
(*S*)-**H1**@[(*S*)-DPEA]$_2$	435 (+49)	421 (-94)	143

[a] In 1.0×10^{-6} M $CHCl_3$ solution at 298 K; λ: peak or trough wavelength in nm; molar extinction coefficients $\Delta\varepsilon = [\theta]/32982$; total amplitude $A_{CD} = \Delta\varepsilon_1 - \Delta\varepsilon_2$ in $mol^{-1}\cdot L\cdot cm^{-1}$.

Table S2. Selected structural parameters from the DFT-optimized structures.[a]

Compound	**Torsion angle** Φ/°	**Interchromophoric distance** R /Å
(*S*)-**H1**	+ 21.22	3.48
(*S*)-**H1**⊃(*R*)-DACH	- 43.18	5.42
(*S*)-**H1**⊃(*S*)-DACH	+ 42.49	5.50
(*S*)-**H1**⊃(*R*)-PPDA	- 31.73	5.18
(*S*)-**H1**⊃(*S*)-PPDA	+ 50.52	6.10
(*S*)-**H1**@[(*R*)-DPEA]$_2$	+ 10.94	4.69
(*S*)-**H1**@[(*S*)-DPEA]$_2$	+ 23.45	4.41

[a] Φ is the spatial angel of C15-C5-C5'-C15'; R is the Zn-Zn distance in Å.

Table S3. The ^{1}H NMR chemical shift (δ, ppm), complexation-induced shift (CIS, $\Delta\delta$, ppm) and chemical shift nonequivalence ($\Delta\Delta\delta$, ppm) values of free and bound (*R*)-/(*S*)-PPDA (0.56 mM) in the presence of (*S*)-**H1** (0.75 mM) in $CDCl_3$ at 298 K.

Proton	Free (*R*)-PPDA δ	(*S*)-**H1**⊃(*R*)-PPDA δ ($\Delta\delta_1$)	(*S*)-**H1**⊃(*S*)-PPDA δ ($\Delta\delta_2$)	$\Delta\Delta\delta$
N-H	1.25	-6.65 (-7.90)	-6.56 (-7.81)	0.09
N-H'	1.25	-7.17 (-8.42)	-7.47 (-8.72)	0.30
H^1	2.82	-5.01 (-7.83)	-4.81 (-7.63)	0.20
H^2	2.78	-6.00 (-8.78)	-6.14 (-8.92)	0.14
H^3	2.97	-5.15 (-8.12)	-5.41 (-8.38)	0.26
H^4	2.55	-2.29 (-4.84)	-2.03 (-4.58)	0.26
H^5	2.49	-3.41 (-5.90)	-3.31 (-5.80)	0.10

[a] $\Delta\delta = \delta_{bound} - \delta_{free;}$ [b] $\Delta\Delta\delta = |\Delta\delta_1 - \Delta\delta_2|$.

Table S4. The ^{1}H NMR chemical shift (δ, ppm) and complexation-induced shift (CIS, $\Delta\delta$, ppm) values of free and bound (*R*)-/(*S*)-PPDA (0.75 mM) in the presence of (*S*)-**H1** (0.75 mM) in $CDCl_3$ at 298 K.

Proton	Free (*R*)-DPEA δ	Bound (*R*)-DPEA δ ($\Delta\delta_1$)	Bound (*S*)-DPEA δ ($\Delta\delta_2$)
N-H	1.55	-2.96 (-4.51)	-2.73 (-4.28)
H^1	4.11	-0.88 (-4.99)	-0.74 (-4.85)

[a] $\Delta\delta = \delta_{bound} - \delta_{free}$.

Reference:

[S1] Zhang, X. Y.; Li, Y.; Qi, D. D.; Jiang, J. J.; Yan, X. Z.; Bian, Y. Z. *J. Phys. Chem.B.*, **2010**, *114*, 13143-13151.

[S2] Thordarson, P., Determining association constants from titration experiments in supramolecular chemistry. *Chem. Soc. Rev.* **2011,** 40, (3), 1305-1323

[S3] Frisch M., Trucks G., Schlegel H., Scuseria G., Robb M., Cheeseman J., et al. Gaussian 09, Revision D.01. Wallingford, CT: Gaussian Inc.; **2013**.